

ANALYSIS OF THE CONTRIBUTION OF AEROSOLS IN OMEGA AND CRISM OBSERVATIONS OF THE POLAR REGIONS OF MARS M. Vincendon, Y. Langevin, F. Poulet, J.-P. Bibring and B. Gondet, Institut d'Astrophysique Spatiale, CNRS/Université Paris Sud, Orsay, France, mathieu.vincendon@ias.u-psud.fr.

Introduction: The observations of the polar regions of Mars in the near-IR by OMEGA have provided important results in the seasonal evolution of surface properties such as ice composition, dust contamination of the ice, and the mean distance between scattering interfaces which is linked to grain size [1, 2, 3, 4]. Martian aerosols significantly scatter the light in the near-IR wavelengths [5]. Near-IR observations of the martian surface from spacecraft therefore contain information about both the surface and the aerosols. We present methods to separate the respective contribution of surface and aerosols in the [1 μm – 2.65 μm] wavelength range of OMEGA and CRISM. These methods have been applied to retrieve surface spectra and to obtain optical depths of dust aerosols above the polar regions of Mars. We perform the modeling of the contribution of dust aerosols between 1 μm and 2.65 μm with a Monte-Carlo based model of radiative transfer [6] and with optical properties previously inferred [7, 6].

Optical depth at 2.63 μm : The south seasonal cap of Mars is mainly constituted of CO_2 ice which present a saturated band at 2.6 – 2.65 μm for most observations. The reflectance at 2.63 μm measured by OMEGA above CO_2 ice-covered surfaces is higher than ~ 0.03 whereas incoming solar photons should be totally absorbed by the surface CO_2 ice. This is mainly due to scattering events on dust that occurs before photons reach the ice. We have demonstrated that the contribution of the surface dust is negligible at 2.63 μm over a major fraction of the south seasonal cap [8]. The most conspicuous exception is the cryptic region which is heavily contaminated by surface dust in mid-spring [9]. As no absorption features by CO_2 gas occur before 2.65 μm , we can use the reflectance at 2.63 μm to map the total optical depth of dust aerosols above regions covered with CO_2 ice free of surface dust contamination. An example of mapping is provided in Figure 1: the regions of the cap with high altitudes ($> 3\text{-}4$ km), near the pole, present low optical depths (0.15 – 0.20). Such low optical depths are also observed in outer regions of the cap ($\sim 70^\circ\text{S}$) although the elevation is significantly lower (~ 1 km). This observation is not compatible with dust well-mixed with the atmosphere and it implies a local process that reduces the loading of dust in the atmosphere. Water ice clouds are observed by OMEGA in outer regions of the seasonal

cap at the beginning of the southern spring [10]. A possible hypothesis for explaining these low optical depths is that dust is scavenged by water condensation. The surface ice spectra observed below these regions of low optical depths are typical of an intimate mixture of dust grains within the ice layer, which support this explanation. This process has been proposed by previous authors as a possible explanation for the low density of absorptive clouds seen by MOLA near the pole [11]. Regions with a large dust optical depth that change in shape and position within in a few days are observed (see regions at $\sim 80^\circ\text{S}$, 300°E in Figure 1). They correspond to dust clouds.

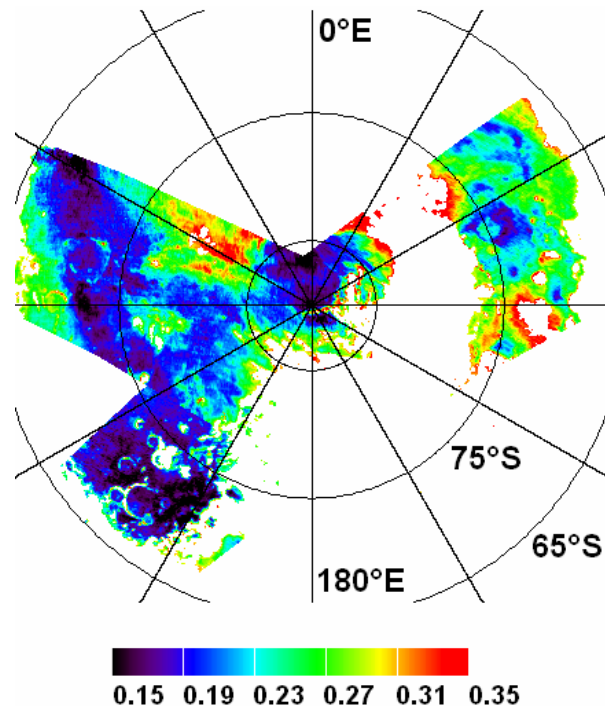


Figure 1: Map of the normal optical depth of dust aerosols at 2.63 μm (L_S 222 $^\circ$) above regions of the south seasonal cap covered with CO_2 ice free of surface dust contamination.

We have determined the variations of the optical depth of dust aerosols above the south perennial cap (87°S) for a period covering southern spring and summer (Figure 2). The strong increase of the optical depth seen by PanCam/Opportunity at mid-latitude [12] at $L_S \sim 320^{\circ}$ is also seen by OMEGA above the south pole.

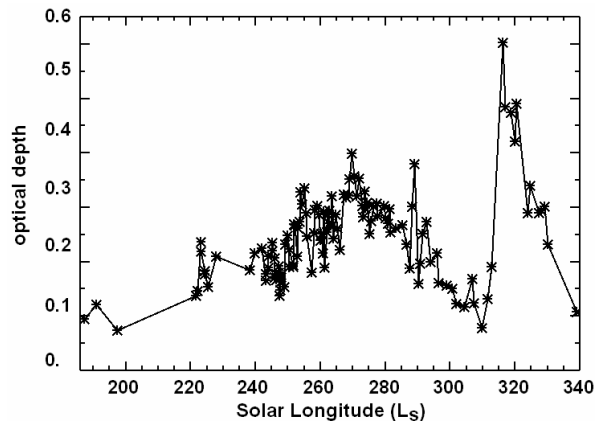


Figure 2: Variations of the optical depth of atmospheric dust at $2.63 \mu\text{m}$ above the south perennial cap (87°S) during southern spring and summer of 2005.

The optical depth of atmospheric dust can not be determined with the $2.63 \mu\text{m}$ reflectance level when the surface is contaminated by dust (e.g. in the cryptic region). Observations of the same surface element with different lighting conditions make it possible to determine the aerosols contribution in such situations [6, 13].

EPF sequences: OMEGA has obtained more than ten Emission Phase Function sequences (EPF, during which the same surface element is observed with different photometric angles). Three of them occur above the polar regions of Mars. It is possible to reproduce the major variations of the Reflectance Factors during these sequences by adjusting only two parameters: the Lambert albedo of the surface and the optical depth of aerosols [13]. OMEGA has recently acquired an EPF sequence above the cryptic region (81°S , $\sim 162^{\circ}\text{E}$) at $L_S 213^{\circ}$ (orbit $n^{\circ} 4168$, April 4th 2007). The major variations of the reflectance factor during the sequence are interpreted as variations of the aerosols contribution which depends on photometric angles (Figure 3).

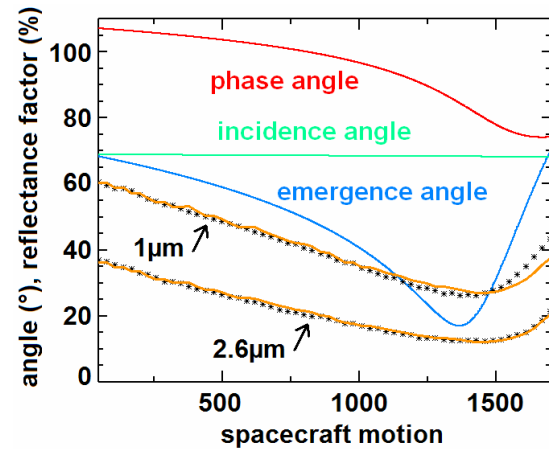


Figure 3: EPF sequence of orbit $n^{\circ} 4168$. The evolution of the photometric angles is indicated in red (phase), blue (emergence) and green (incidence). The observed variations of the reflectance factor are indicated in black for two wavelengths ($1 \mu\text{m}$, corresponding to the continuum of the ice spectrum, and $2.6 \mu\text{m}$ in an absorption band). A satisfactory model fit (yellow lines) is obtained with $\tau=0.57$ and $A_L=0.2$ for $1 \mu\text{m}$ and with $\tau=0.29$ and $A_L=0.06$ for $2.6 \mu\text{m}$.

A northern region covered by water ice (232.5°E , 74.75°N) at $L_S 57.7^{\circ}$ (May 26th 2006) as been observed during orbit $n^{\circ}3049$ [13]. This EPF sequence has been used to retrieve the spectrum of the surface without contribution of aerosols (Figure 4). It is very consistent with the expected spectrum of small-grained water ice [2, 3].

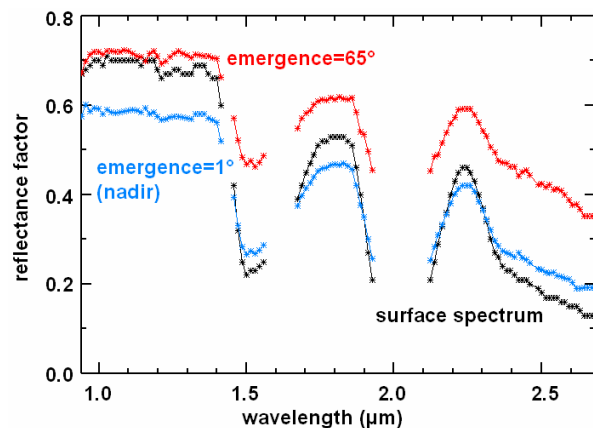


Figure 4: Near-IR spectra of a surface covered with water ice during the EPF sequence of orbit $n^{\circ}3049$ (red and blue). The surface spectrum without aerosols contribution obtained with our model is indicated in black.

CRISM is providing an EPF sequence for each targeted observation [14]. These EPF sequences will be used to retrieve aerosols properties [15] and Lambert albedos of the surface [16]. An example of CRISM EPF sequence analyzed with our approach is indicated in Figure 5.

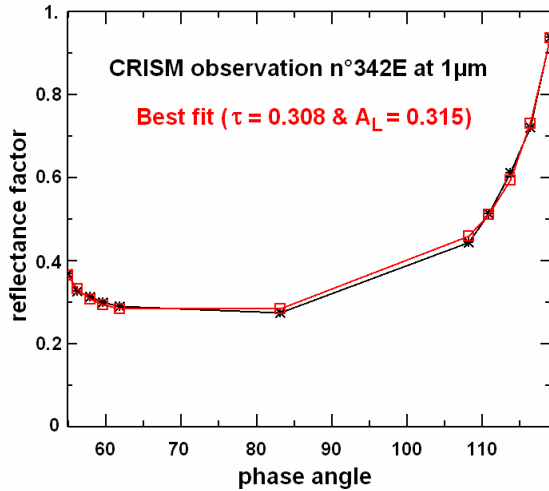


Figure 5: CRISM EPF sequence n°342E at 1 μm (black stars). The best fit of this sequence with our model is indicated in red squares. It is obtained for an optical depth of 0.308 and a Lambert albedo of the surface of 0.315.

Terminator: An intensive observation campaign of the south polar cap of Mars have been achieved by OMEGA and CRISM during the late winter and the early spring of 2007. These observations will be used to enhance our comprehension of the development of the cryptic region of Mars [4, 17]. Near the pole, the sun elevation is restrained to a few degrees during this period. The path of incident photons in the layer of aerosols is proportional to $1/\cos(\text{incidence angle})$. Close to the terminator, most photons have interacted with aerosols before reaching the surface or the spacecraft. CO₂ ice signatures are observed by OMEGA up to five degrees beyond the terminator (Figure 6). This demonstrate that the surface is illuminated by photons scattered by aerosols.

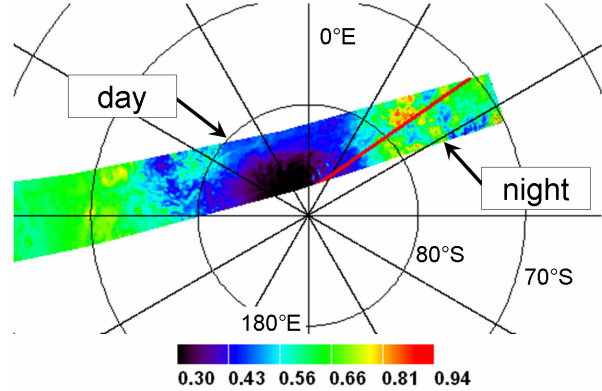


Figure 6: Map of the 1.43 μm band strength of surface CO₂ ice. The terminator line is indicated (red line). The surface signature of CO₂ ice is clearly detected for incidences up to 95° due to photons scattered by aerosols toward the surface in the night side.

A plan parallel hypothesis is not appropriate for analyzing such a situation. We have developed a model of radiative transfer with a spherical geometry so as to account for observations at the terminator. This model can predict the flux received by the surface and the flux directly scattered by aerosols toward the instrument. The surface has been observed after the terminator during orbit n° 41 (Figure 7). It is possible to obtain a good fit of the variations of the flux measured as a function of the solar incidence angle for reasonable parameters. The predictions of the model strongly depends on the assumed vertical distribution of dust in the atmosphere.

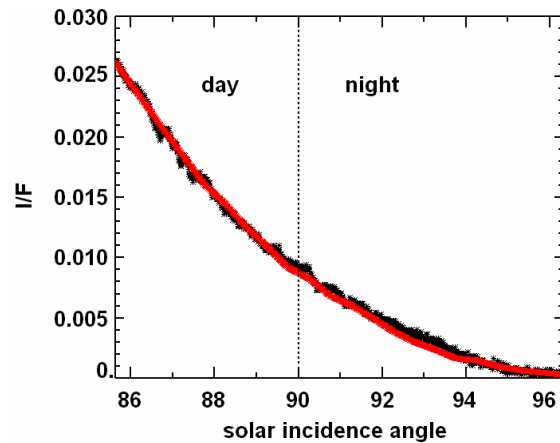


Figure 7: Variations of I/F at 1.7 μm with the solar incidence angle around the terminator (black, orbit 41, 280°E, 72°S-83°S). These variations are modeled (red) with a surface albedo of 33% and an optical depth of aerosols of 0.13.

Conclusion: The Monte-Carlo approach we have selected for assessing the contribution of aerosols to near-IR Mars spectra makes it possible to model a wide range of illumination conditions. Using observations obtained with different photometric angles, we have validated a method of mapping of the optical depth of aerosols which lies on the reflectance at 2.63 μm . EPF sequences for both OMEGA and CRISM can be interpreted by adjusting only two parameters: the albedo of the surface and the optical depth of aerosols. An important point is that until now we have been able to interpret most cases with a simple Lambert assumption for the surface photometric properties at moderate phase angles, in agreement with [18]. The Monte-Carlo approach makes it possible to model observations near or beyond the terminator which required a full 3D approach. Improving our understanding of the aerosols contribution is useful for retrieving surface reflectance spectra from OMEGA observations (most with nadir pointing). This issue is particularly critical for high resolution CRISM observations at high latitudes with phase angles varying by up to 70°.

References: [1] Bibring J.-P. et al. (2004) *Nature*, 428, 6983, 627-630. [2] Langevin Y. et al. (2005) *Science*, 307, 1581 [3] Douté S. et al. (2007) *Planet. Space Sci.* 55, 113–133. [4] Langevin et al. (2007) *this conference* [5] Erard S. (1994) *Icarus*, 111, 317-337 [6] Vincendon M. et al. (2007), *JGR*, in press. [7] Ockert-Bell M.E (1997) *JGR.*, 102(E4), 9039-9050. [8] Vincendon M. et al. (2007) *LPSC XXXVIII*, Abstract #1665. [9] Langevin et al. (2006) *Nature*, 442, 831-835. [10] Langevin et al. (2007), *JGR*, in press. [11] Neumann G. A. et al. (2003) *JGR.*, 108(E4), 4-1, 5023 [12] Lemmon M. T. (2004), *Science*, 306, 1753-1756. [13] Vincendon M. et al. (2007) *LPSC XXXVIII*, Abstract #1650. [14] Murchie S. et al. (2007) *LPSC XXXVIII*, Abstract #1472. [15] Wolff M. J. et al. (2006), *AGU*, P23B0060. [16] McGuire P. C. et al. (2006) *LPSC XXXVII*, Abstract #1529. [17] Langevin et al. (2007) *LPSC XXXVII*, Abstract #1602. [18] Johnson J. R. et al. (2006) *JGR*, 111(E2), E02S14.